RAPID COMMUNICATIONS

PHYSICAL REVIEW B VOLUME 48, NUMBER 3 15 JULY 1993-I

Microscopic origin of optical nonlinearities associated with excitations between valence minibands in p-type GaAs-AlAs and Si-$Si_{1-x}Ge_x$ heterostructures

M. J. Shaw, K. B. Wong, and M. Jaros

Department of Physics, The University of Newcastle upon Tyne, Newcastle upon Tyne, United Kingdom

(Received 14 April 1993)

We have carried out full-scale semi-empirical relativistic pseudopotential calculations of the frequency dependence—spanning the midinfrared to far infrared range of frequencies—of $\chi^{(2)}(-2\omega;\omega,\omega)$ associated with excitations between valence minibands in p-type GaAs-AlAs and Si-SiGe heterostructures. We find that the spectrum is dominated by excitations lying further from the center of the Brillouin zone and depends on states lying above the semiclassical barrier.

It is well known that oscillator strengths of optical transitions between adjacent minibands in semiconductor heterostructures are large and that the miniband separations can be tuned over a significant range of energies spanning the midinfrared to far infrared range of wavelengths.[1] Since several minibands can often be confined within a sufficiently deep well these structures offer an opportunity to study not only linear (first-order) susceptibility but also nonlinear (higher-order) effects in which several virtual excitations occur.[2–4] Of particular interest is the understanding of the microscopic origin of the optical spectra, i.e., the actual processes on which the strength and the frequency at the peak value of the optical effect depend. This establishes a link between the structural and electronic properties which could be used to tune and optimize the strength of the optical response, its frequency, and the directional dependence. For example, transitions between the lowest conduction minibands in direct-gap heterostructures require the incoming beam to lie in the plane of the interface. Such a geometrical arrangement is inconvenient for practical applications. The situation is different in the valence band where the mixing between bulk light- and heavy-hole states brought about by the change of symmetry and by the strength of the crystal potential of the heterostructure in question may make the selection rules for optical transition probabilities more advantageous.[5] However, the structure of the valence band is more complex, particularly in strained systems. This is especially relevant in the case of higher-order susceptibilities. For example, for the second-order susceptibility to be large three transitions must be strong, at least one of which must of necessity connect states that are not adjacent to each other. The dipole matrix element between such states is either zero or small. However, mixing of bulklike valence-band wave functions by strain and by the axial potential created in a suitably chosen heterostructure (e.g., steplike or otherwise asymmetric wells) may enhance such weak transitions without reducing significantly the allowed processes. It is the purpose of this study to identify the microscopic origin of the processes dominating the second-order susceptibility with a view to providing a theoretical and quantitative basis for experimentation with optical nonlinearities in such structures. In particular, we present a full-scale evaluation of both GaAs-AlAs and Si-SiGe quantum-well structures in which the nonlinearities arise due to virtual optical transitions between valence minibands. Steplike wells have been used to modify the structure of confined states and to enhance the second harmonic generation in the $3-5$- and $10-15$-μm range, respectively.

The process of second harmonic generation is described by the second-order susceptibility tensor $\chi^{(2)}(-2\omega;\omega,\omega)$. Using the density matrix theory,[6] the following expression for $\chi^{(2)}(-2\omega;\omega,\omega)$ is obtained:

$$\chi^{(2)}_{\mu\alpha\beta}(-2\omega;\omega,\omega)=\frac{-ie^3}{\epsilon_0 V 2\hbar m^3 2\omega^3}\sum_{abc}\sum_{k} f_0(a,k)\left[\frac{p^{\mu}_{ab}p^{\alpha}_{bc}p^{\beta}_{ca}+p^{\mu}_{ab}p^{\beta}_{bc}p^{\alpha}_{ca}}{(\Omega_{ba}-i\Gamma_{bc}-i\Gamma_{ca}-2\omega)(\Omega_{ca}-i\Gamma_{ca}-\omega)}\right.$$
$$+\frac{p^{\alpha}_{ab}p^{\mu}_{bc}p^{\beta}_{ca}+p^{\beta}_{ab}p^{\mu}_{bc}p^{\alpha}_{ca}}{(\Omega_{ba}+i\Gamma_{ba}+\omega)(\Omega_{ca}-i\Gamma_{ca}-\omega)}$$
$$\left.+\frac{p^{\beta}_{ab}p^{\alpha}_{bc}p^{\mu}_{ca}+p^{\alpha}_{ab}p^{\beta}_{bc}p^{\mu}_{ca}}{(\Omega_{ba}+i\Gamma_{ab}+\omega)(\Omega_{ca}+i\Gamma_{ab}+i\Gamma_{bc}+2\omega)}\right], \tag{1}$$

where the component $\chi^{(2)}_{\mu\alpha\beta}(-2\omega;\omega,\omega)$ describes the second harmonic polarization induced in the μ direction (i.e., in the direction which the induced electric-field vector lies) by incident optical fields at frequency ω polarized in the α and β directions. In Eq. (1), $\sum_{abc}$ represents the summation of a, b, and c over all possible states (minibands) at a particular wave vector k. Each combination of abc represents the contribution from the virtual process $a\rightarrow c\rightarrow b\rightarrow a$. Ω_{ij} is the transition frequency between minibands i and j, and p^{δ}_{ij} is the momentum matrix element in the δ direction between i and j. Clearly, for a semiconductor system, the miniband energy separations

0163-1829/93/48(3)/2001(4)/$06.00

and momentum matrix elements will have a wave-vector dependence, and the expressions for the susceptibilities include a summation over a set of randomly chosen sampling points in the superlattice Brillouin zone, $\sum_k$. The Fermi distribution function $f_0(a,k)$ represents the thermal equilibrium populations of the states. Relaxation processes have been included phenomenologically in the form of the damping terms Γ_{ij} in the frequency denominators of Eq. (1). This provides a good description of the response at low intensities.[7] At higher intensities, where significant changes in population take place due to optical pumping, a more sophisticated treatment of the relaxation mechanisms is required. We restrict ourselves to considering the low-intensity behavior. In the absence of any accurate estimates of the damping constants a single linewidth was used for all transitions.

To evaluate the susceptibility of a superlattice from Eq. (1) requires a detailed knowledge of the band structure. For each of the structures studied, a semiempirical relativistic pseudopotential calculation was performed which correctly accounts for the details of the valence minibands throughout the Brillouin zone. The p-type doping in the structures considered results in a Fermi level lying below the valence-band edge. Only a low doping concentration is considered.

The second-order susceptibility of a 5GaAs/$1Al_{0.5}Ga_{0.5}As$/14AlAs superlattice, with p-type doping in the barriers, was calculated using Eq. (1) in the manner described[7,8] in our previous publications. (5GaAs represents 5 monolayers, i.e., 2.5 lattice constants of bulk GaAs.) A schematic level diagram for the structure is shown in Fig. 1, with principal zone center transition energies indicated. The frequency dependence of the five independent nonzero components of $\chi^{(2)}(-2\omega;\omega,\omega)$ were calculated at 0 K. The Fermi level was chosen to lie 65 meV below the superlattice valence-band edge, and is shown in Fig. 2. The damping constant is set to 3 meV to represent a typical heterostructure linewidth. It can be seen that the dominant component is $\chi^{(2)}_{xyz}$, with a maximum value of 4.8×10^{-5} esu at photon energy of 340 meV. From a naive particle-in-a-box model one might have expected that $\chi^{(2)}_{zzz}$ is dominant due to processes of the type HH3→HH2→HH1→HH3 shown in Fig. 3(i) (where HHn refers to the nth heavy-hole miniband). A detailed analysis of the individual processes which contribute to $\chi^{(2)}_{xyz}$ in our calculation indicates that processes of the type shown in Fig. 3(ii) are dominant. In particular, the peak at 340 meV results from processes where

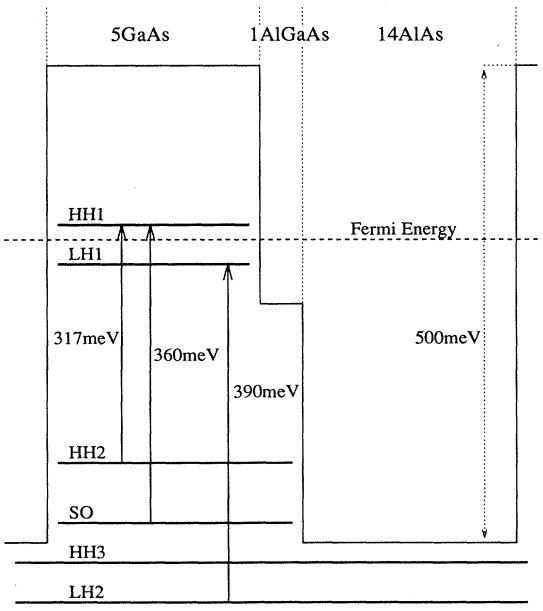

FIG. 1. Schematic energy band diagram of the 5GaAs/$1Al_{0.5}Ga_{0.5}As$/14AlAs superlattice valence band (5GaAs represents 5 monolayers, i.e., 2.5 lattice constants of GaAs). HHn represents the nth heavy-hole miniband, LHn the nth light-hole miniband, and SO the spin split-off miniband. Zone center transition energies between some of the key states are shown.

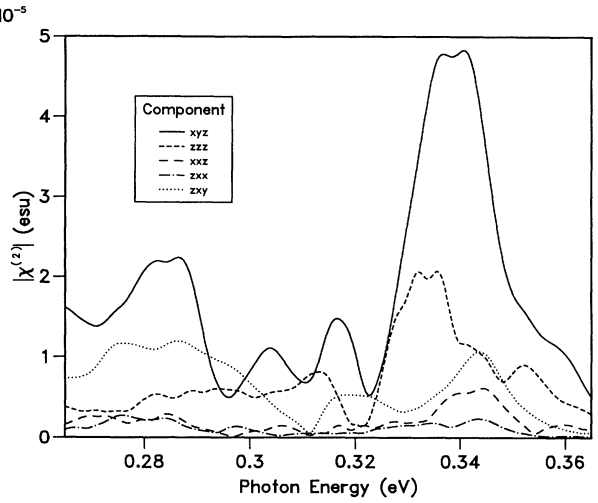

FIG. 2. The magnitude of the five independent components of $\chi^{(2)}(-2\omega;\omega,\omega)$ in esu, plotted against the photon energy in eV, for the p-type 5GaAs/$1Al_{0.5}Ga_{0.5}As$/14AlAs superlattice at 0 K. The component labels $\mu\alpha\beta$ are those in Eq. (1) where z is the superlattice growth direction.

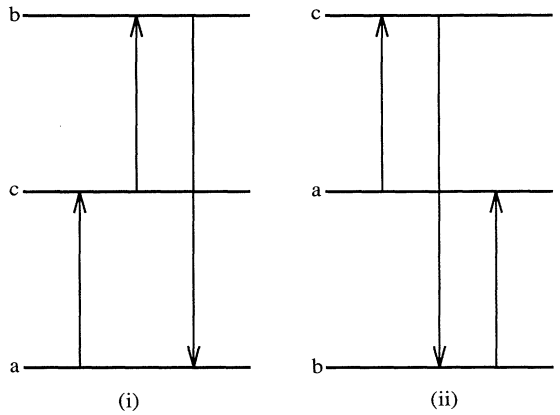

FIG. 3. Schematic diagrams representing two possible processes $a \rightarrow c \rightarrow b \rightarrow a$ which can contribute to the second-order susceptibility, $\chi^{(2)}$. The labels a, b, and c refer to Eq. (1).

a, b, and c represent the spin split-off state (SO), various low-energy continuum states (C), and the ground heavy-hole state (HH1), respectively. Large contributions occur for such processes where the transitions $a \rightarrow c$ and $b \rightarrow a$ are simultaneously resonant with ω, causing the denominator of the second term in Eq. (1) to be small. Our full band-structure calculations, which include the effects of valence-band mixing, thus predict a $\chi^{(2)}$ dominated by different processes to those intuitively expected from simple theory.

From the above discussion it might be expected that the peak value of $\chi^{(2)}$ would occur at 360 meV, the zone-center SO→HH1 energy separation (see Fig. 1). However, the total susceptibility results from the summation of the contributions from k points throughout the Brillouin zone. We find that the momentum matrix element, p_{ij}^{δ} in Eq. (1), is a rapidly varying function of k due to the strong mixing of heavy- and light-hole minibands. p_{ij}^{δ} at the zone center is certainly not representative. For instance, the SO→HH1 transition is stronger, and occurs at lower energies, at k points lying away from the zone center. These points thus dominate the overall response, and result in the position of the peak of the spectrum at lower energy of 340 meV (Fig. 2).

We have also studied the second-order susceptibilities in an analogous Si-SiGe system. The light- and heavy-hole mixing is stronger in this strained-layer superlattice due to strain-induced momentum mixing.[8] This alters the nonlinear optical interactions. The second-order susceptibility was evaluated in a $18Si_{0.85}Ge_{0.15}/2Si_{0.925}Ge_{0.075}/40Si$ superlattice grown on (001) Si substrate (40Si represents 40 monolayers, i.e., 10 lattice constants of Si). A schematic energy level diagram for the structure is shown in Fig. 4, with principal zone center transitions indicated. In Fig. 5 we present the frequency dependence of the five independent nonzero components of $\chi^{(2)}(-2\omega;\omega,\omega)$ evaluated at 0 K for the Fermi level chosen to lie 26 meV below the top of the uppermost valence miniband. The damping constant used corresponds to a linewidth of 1.5 meV. A smaller value is chosen here merely for the purpose of making it easier to resolve better the individual peaks due to different processes and to obtain a better understanding of the role of band-structure effects. However, it should be noted that the magnitude of $\chi^{(2)}$ increases as the magnitude of the damping constant decreases. This is generally true for all susceptibilities.[9]

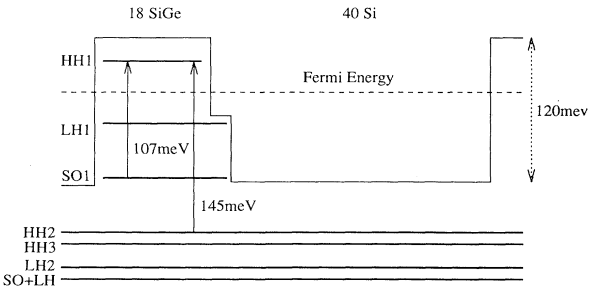

FIG. 4. Schematic energy band diagram of the $18Si_{0.85}Ge_{0.15}/2Si_{0.925}Ge_{0.075}/40Si$ superlattice valence band (40Si represents 40 monolayers, i.e., 10 lattice constants of Si). Zone center transition energies between some of the key states are shown.

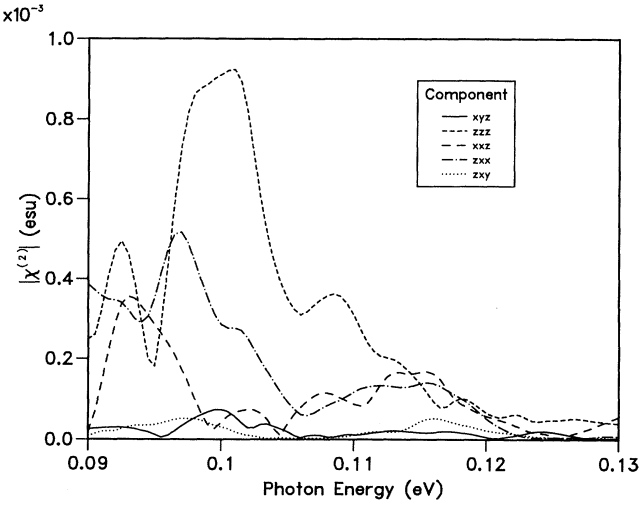

FIG. 5. The magnitude of the five independent components of $\chi^{(2)}(-2\omega;\omega,\omega)$ in esu, plotted against the photon energy in eV, for the p-type $18Si_{0.85}Ge_{0.85}/2Si_{0.925}Ge_{0.075}/40Si$ superlattice at 0 K. The component labels $\mu\alpha\beta$ are those in Eq. (1) where z is the superlattice growth direction.

It is shown in Fig. 5 that the largest component is $\chi_{zzz}^{(2)}$, with a maximum value of 9.5×10^{-4} esu at photon energy of 100 meV. The processes which dominate the contributions to this peak are identified to be C→SO→HH1→C and SO→HH1→C→SO. The states are labeled in the same manner as in the GaAs-AlAs system. These two processes have been described earlier in Fig. 3. Unlike the GaAs structure here both processes are equally important. There are two other satellite peaks near the central peak. The peak lying at energy of 93 meV is dominated by the same processes. Apparently, the peak at higher energy of 107 meV corresponds to the zone center SO→HH1 energy separation (see Fig. 4). However, we find two additional contributions apart from those mentioned above, namely, C→HH2→HH1→C and HH2→HH1→C→HH2. The transition energy between HH1 and HH2 at the edge of the superlattice Brillouin zone (in the z direction) is also 107 meV. In fact, the magnitude of such a peak cannot be predicted without including contributions from all the possible transitions associated with various intersubband processes. The argument invoked above, namely, that the momentum mixing is only strong away from the zone center, can be applied here too. It results in an energy shift of the largest peak at 100 meV. Such shifts are even more prominent in components $\chi_{zxx}^{(2)}$ and $\chi_{xxz}^{(2)}$ which both peak at energies further away from the zone center transition energy of SO→HH1 (95 meV for $\chi_{zxx}^{(2)}$ and 92 meV for $\chi_{xxz}^{(2)}$ as shown in Fig. 5).

The strength of the optical transition matrix elements is an important factor in determining the magnitude of the peaks. It is governed by the degree of light- and heavy-hole mixing in the states concerned. It is found

that the mixing is strongest for state SO when transition SO→HH1 occurs at 100 meV. We also find that the component $\chi^{(2)}_{zxx}$ has a large magnitude of 5×10^{-4} esu at 95 meV. $\chi^{(2)}_{zxx}$ describes an induced polarization in the z direction in response to fundamental fields applied in the x direction (parallel to the interfaces). This component is therefore particularly useful for device application as incident light is polarized in the plane parallel to the superlattice layers (i.e., the velocity vector lies along the growth axis perpendicular to the plane of the interfaces, see Fig. 6). Finally, it is worth pointing out that the key transition SO→HH1 is responsible for the largest peak in $\chi^{(2)}$ for both systems discussed above, but the peaks correspond to a different component. For example, the largest component $\chi^{(2)}_{xyz}$ in the GaAs-AlAs system becomes very small in the Si-SiGe system. It shows that the band-structure effects also influence the directional properties of the nonlinear optical response.

In this account of our calculations we have not been able to discuss a number of approximations adopted in our procedure which, because of their highly technical character, lie outside the format of this paper. These include, in particular, the absence of finite-temperature results, the treatment of many-body corrections (which we incorporated roughly in line with the prescription available in the literature[10]), the cavalier choice of the "damping" constants in Eq. (1), the uncertainties in the details of the curvature of the valence minibands and the corresponding uncertainties in the density of states, the accuracy with which our computer codes evaluate the weak near-forbidden optical matrix elements which are nevertheless important in the total summations over the many different processes made available by the changes in the selection rules due to, say, strain in SiGe, etc. We have also ignored the possibility of interdiffusion and other deviations from perfect geometry of the system all of which might affect the sharp features in the predicted spectra. We are confident that in our experience none of these idealizations are serious enough to alter the main conclusions of our study, namely, the identification of the main process and the nontrivial relation (shift) between the conventional zone center energy level diagram and the position of the spectral peaks. We believe that the relevant corrections would in the main broaden the spectra presented in this study. However, it is clear that more work needs to be done before a definitive statement concerning the spectral form of second-order processes in these systems can be made.

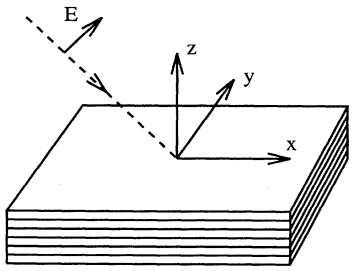

FIG. 6. The dashed line represents the direction of propagation of a beam of light incident at some general angle to the superlattice surface. For a practical device the preferred direction of propagation is normal to the surface, i.e., with velocity component parallel to the z axis and electric field E parallel to the interfaces.

In conclusion our calculations show that significant second harmonic generation is possible due to inter-valence miniband transitions in p-type asymmetric quantum-well structures, with favorable directional properties. $\chi^{(2)}(-2\omega;\omega,\omega)$ as large as 4.8×10^{-5} esu in the GaAs-AlAs system and 9.5×10^{-4} esu in the Si-SiGe system were obtained. We find that contrary to the intuitive picture of the excitation process HH1-HH2-HH3 does not dominate the spectra. The position of the peak response depends mainly on excitations lying away from the center of the Brillouin zone and involves higher-lying minibands.

We would like to thank the United Kingdom Science and Engineering Research Council, the Office of Naval Research (USA), and ESPRIT-Basic Research European Community Programme for financial support.

[1] B. F. Levine, K. K. Choi, C. G. Bethea, J. Walker, and R. J. Malik, Appl. Phys. Lett. **50**, 1092 (1987).
[2] C. Sirtori, F. Capasso, D. L. Sivco, and A. Y. Cho, Phys. Rev. Lett. **68**, 1010 (1992).
[3] L. Tsang and S. L. Chuang, Appl. Phys. Lett. **60**, 2543 (1992).
[4] X. H. Qu and H. Ruda, Appl. Phys. Lett. **62**, 1946 (1993).
[5] Y. C. Chang and R. B. James, Phys. Rev. B **39**, 12672 (1989).
[6] P. N. Butcher and D. Cotter, *The Elements of Nonlinear Optics* (Cambridge University Press, England, 1990).
[7] M. J. Shaw, D. Ninno, B. M. Adderley and M. Jaros, Phys. Rev. B **45**, 11031 (1992).
[8] I. Morrison, M. Jaros, and K. B. Wong, Phys. Rev. B **18**, 9693 (1987).
[9] S. L. Chuang, S. Schmitt-Rink, B. I. Greene, P. N. Saeta, and A. F. J. Levi, Phys. Rev. Lett. **68**, 102 (1992).
[10] K. M. S. V. Bandara, D. D. Coon, Byungsung O, Y. F. Lin, and M. H. Francombe, Appl. Phys. Lett. **53**, 1931 (1988).